ITUPublications

International Telecommunication Union
Radiocommunication Sector

# Report ITU-R P.2553-0

**(06/2025)**

P Series: Radiowave propagation

# Measurements of radio frequency characteristics of building materials

## Foreword

The role of the Radiocommunication Sector is to ensure the rational, equitable, efficient and economical use of the radio-frequency spectrum by all radiocommunication services, including satellite services, and carry out studies without limit of frequency range on the basis of which Recommendations are adopted.

The regulatory and policy functions of the Radiocommunication Sector are performed by World and Regional Radiocommunication Conferences and Radiocommunication Assemblies supported by Study Groups.

## Policy on Intellectual Property Right (IPR)

ITU-R policy on IPR is described in the Common Patent Policy for ITU-T/ITU-R/ISO/IEC referenced in Resolution ITU-R 1. Forms to be used for the submission of patent statements and licensing declarations by patent holders are available from https://www.itu.int/ITU-R/go/patents/en where the Guidelines for Implementation of the Common Patent Policy for ITU-T/ITU-R/ISO/IEC and the ITU-R patent information database can also be found.

### Series of ITU-R Reports

(Also available online at https://www.itu.int/publ/R-REP/en)

| Series | Title |
|---|---|
| **BO** | Satellite delivery |
| **BR** | Recording for production, archival and play-out; film for television |
| **BS** | Broadcasting service (sound) |
| **BT** | Broadcasting service (television) |
| **F** | Fixed service |
| **M** | Mobile, radiodetermination, amateur and related satellite services |
| **P** | **Radiowave propagation** |
| **RA** | Radio astronomy |
| **RS** | Remote sensing systems |
| **S** | Fixed-satellite service |
| **SA** | Space applications and meteorology |
| **SF** | Frequency sharing and coordination between fixed-satellite and fixed service systems |
| **SM** | Spectrum management |
| **TF** | Time signals and frequency standards emissions |

***Note****: This ITU-R Report was approved in English by the Study Group under the procedure detailed in Resolution ITU-R 1.*

*Electronic Publication*
Geneva, 2025

# REPORT ITU-R P.2553-0

# Measurements of radio frequency characteristics of building materials

(2025)

**Scope**

This Report provides a compilation of measurement data relating to the electrical characteristics of building materials. It is intended to supplement the material in Recommendation ITU-R P.2040.

TABLE OF CONTENTS

*Page*



## 1 Introduction

This Report provides a compilation of empirical measurement data relating diverse materials and is intended to support the material in Recommendation ITU-R P.2040.

## 2 Reflection and penetration loss of building materials at 28 GHz and 39 GHz

### 2.1 Measurements setup and procedures

In the literature, measurements of reflection and transmission loss for a number of common building materials have been reported in different mmWave bands, such as the 26.5 to 40 GHz bands in [2], the 28 GHz band in [3], [4], the 38 GHz band in [4], the 60 GHz band in [1], and the 73 GHz band in [5]. Preceding experiments have shown that penetration and reflection loss are influenced by different factors such as the thickness of the material, the incident angle, temperature, humidity and frequency.

Most of the previous work has been performed within buildings, where the measurements were not under the same conditions for all the tested materials. The current measurements were performed at 28 GHz and 39 GHz using the wideband chirp (FMCW) channel sounder [6] with two different set ups: one for the penetration loss and one for reflection loss measurements. The channel sounder parameters are given in Table 1. In contrast to continuous wave (CW) measurements, the wideband measurements give processing gain and high time delay resolution which provides further information on the material properties.

TABLE 1

**Channel sounder parameters**

| | |
|---|---|
| Centre frequency (GHz) | 28, 39 |
| Measurement BW (GHz) | 3, 4.5 |
| Processing BW (GHz) | 2 |
| Sampling rate (MHz) | 40 |
| Sweep rate (kHz) | 1.22 |
| Link polarization | VV, HV |
| Tx, Rx antenna (gain, beam) | Lens horn (20 dBi, 4.5º) |
| Tx (Rx) antenna height (m) | 1.42 |
| Tx-Rx distance(m) | 1.9 |
| Record duration (s) | 1 |

The penetration loss measurements for several common building materials listed in Table 2, were performed for co-polar (VV) and cross-polar (HV) antenna alignment. The penetration loss measurements were conducted with different incidence angles from −30 degrees to +30 degrees with 5 degree steps as shown in Fig. 1(a), where at zero angle the antenna was perpendicular onto the building material. To measure the penetration loss (PenL), the measurements were performed with the material present between the transmitter and receiver (PRm) and without the material (FSPL), where the penetration loss equals the difference between the two measurements as in equation (1).

$$PenL = PRm - FSPL \tag{1}$$

The reflection loss measurements were conducted with different angles (15, 25, 35, 45 and 55 degrees), where the transmitter and receiver antennas were both lens antennas with (4.5 degrees) beamwidth and were placed at mirroring angles from the perpendicular on the same side of the tested material as shown in Fig. 1(b) setup in the chamber.

TABLE 2

**Material dimensions**

| Material | Width (mm) | Hight (mm) | Thickness (mm) |
|---|---|---|---|
| Plexiglass | 1 200 | 600 | 4 |
| Hardboard | 1 220 | 610 | 3 |
| Plasterboard | 1220 | 600 | 12.5 |
| MDF board | 1 220 | 610 | 12 |
| Glass | 1 000 | 600 | 4 |
| Wood flooring | 1 220 | 600 | 15 |

FIGURE 1

**Measurement environments and layout for penetration and reflection loss**

(a) Principle of transmission measurement (penetration loss)

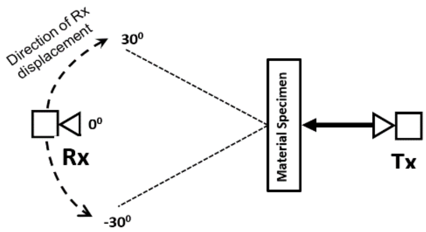


(b) Principle of reflection measurement

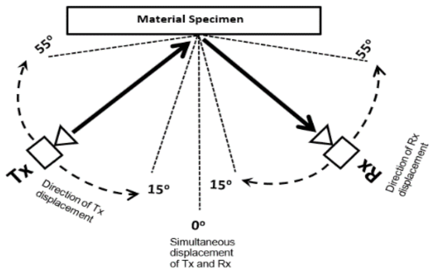


(c) Measurement setup in anechoic chamber

A sample of double-glazed window with a width of 1 000 mm and length of 600 mm was added for the reflection loss measurements. To perform the reflection measurements a sheet of aluminium was taken as a reference (considered a total reflector). The measurements were conducted (in co-polar (VV) and cross-polar (HV) antenna alignment) with the aluminium first (PRref) then replaced by the building material (PRm). The reflection loss (RL) was then calculated as the difference between the two measurements as shown in equation (2), with 0 dB corresponding to total reflection.

$$RL = PRm - PRref \quad (2)$$

FIGURE 2

**Measured power delay profiles at 28 GHz cross-polar at 90° incident angle**
**(a) Free space, (b) Wood flooring**

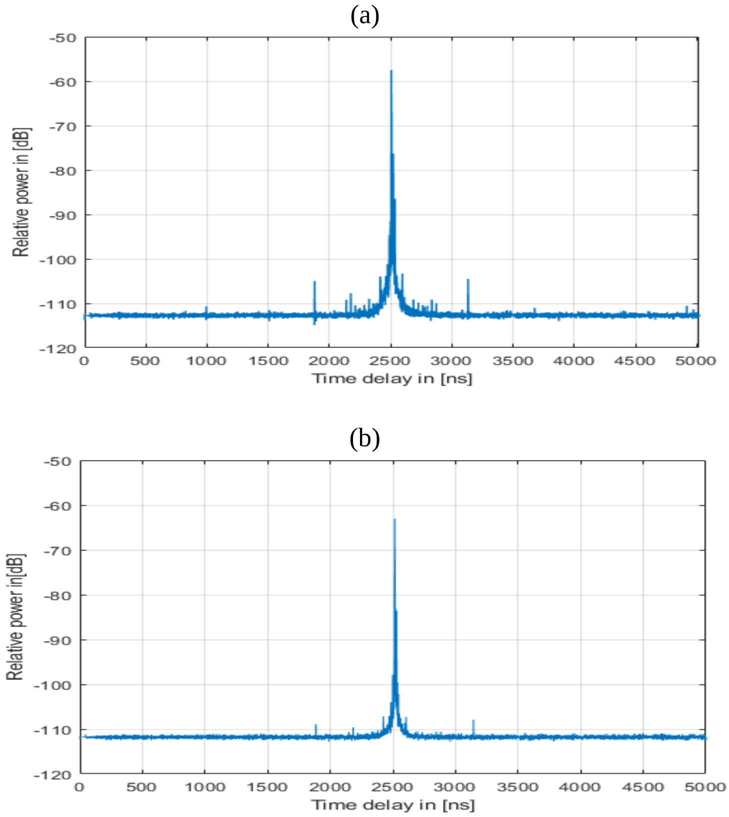


## 2.2 Measurement results and analysis

The collected data were processed with 2 GHz bandwidth for both bands to obtain the power delay profile (PDP) at each angle for both measurement setups for each tested material then used to estimate the received power which is then used to calculate the penetration loss and reflection loss.

### 2.2.1 Penetration loss

Figure 2 presents the measured PDPs at 28 GHz for cross-polar (HV) alignment at 90° incident angle without material in (a) and with wood flooring in (b) which shows the difference in the power level between the two PDPs due to the penetration loss in wood flooring material.

Figure 3 presents the penetration loss against the incident angles for all the tested materials at the 28 GHz and 39 GHz bands in co-polar and cross-polar alignments. The cross-polar alignment for both bands have, in general, lower penetration loss values over the incident angles compared to the co-polar. The penetration loss was more than 20 dB in the cross-polar alignment for most of the tested materials at angles larger than 10 degrees on either side from the zero angle, while it was more than 30 dB in the co-polar alignment. There is similarity in the transmission loss values over the angles between the glass and plexiglass and between the hardboard, MDF board and plasterboard. The wood flooring shows lower penetration loss variation as the incident angle moves away from the zero-incident angle at both sides compared with the other tested materials, where it was within 40 dB for all angles. The results in Table 3 show an increase in penetration loss at 0 degree incident angle as the frequency increases.

FIGURE 3

**Penetration loss vs incident angle for all materials at 28 GHz and 39 GHz in co-polar (VV) and cross-polar (HV) alignments**

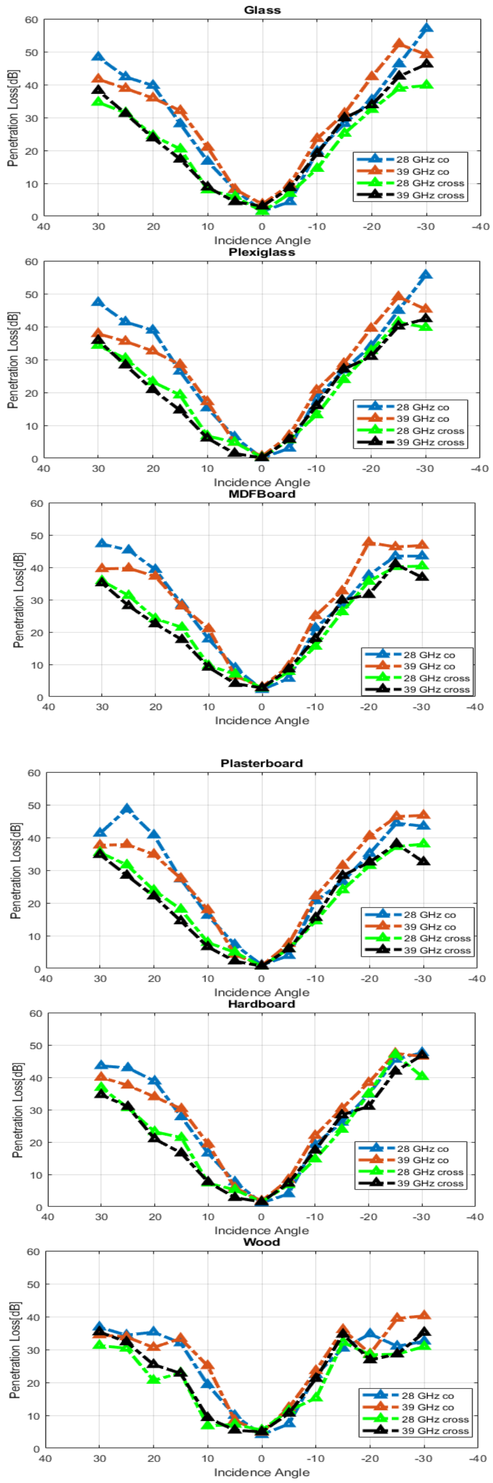

TABLE 3

**Estimated penetration loss, in dB, at 0° incident angle**

| Material | Polar | 28 GHz | 39 GHz |
|---|---|---|---|
| Glass | VV | 1.49 | 3.65 |
| | HV | 1.39 | 3.05 |
| Plexiglass | VV | 0.09 | 0.55 |
| | HV | 0.23 | 0.11 |
| Hardboard | VV | 1.18 | 1.77 |
| | HV | 1.51 | 1.51 |
| Plasterboard | VV | 1 | 0.83 |
| | HV | 0.66 | 0.69 |
| MDF board | VV | 2.18 | 2.95 |
| | HV | 2.63 | 2.74 |
| Wood flooring | VV | 4.11 | 4.81 |
| | HV | 5.49 | 4.98 |

### 2.2.2 Reflection loss

Figure 4 displays the reflection loss for all tested materials for co-polar and cross-polar alignments. In general, the tested materials show lower loss reflection variation at the 39 GHz band compared with the 28 GHz band, where the reflection loss was whin 16 dB and 30 dB respectively. The double-glazed window was highly reflective over most of the angles especially in the cross-polar (HV) at both bands, where it was higher than the reference material (positive values). The glass was the second high reflective material for both bands. For the 28 GHz band the plexiglass shows the lowest reflection values compared with the other materials, where the lowest values were at the 35° incident angle. At 39 GHz the wood and MDF boards display the lowest reflection values for both co- (VV) and cross-polar (HV) for most of the angles. It can be noticed that there is remarkable change in the reflection values for most of the tested materials at the angle of 35 degrees.

FIGURE 4

**Reflection loss vs incident angles for all measured materials: (a) co-polar (VV) and (b) cross-polar (HV) at 28 GHz, respectively and (c) co-polar (VV) and (d) cross-polar (HV) at 39 GHz, respectively**

(a) (b)

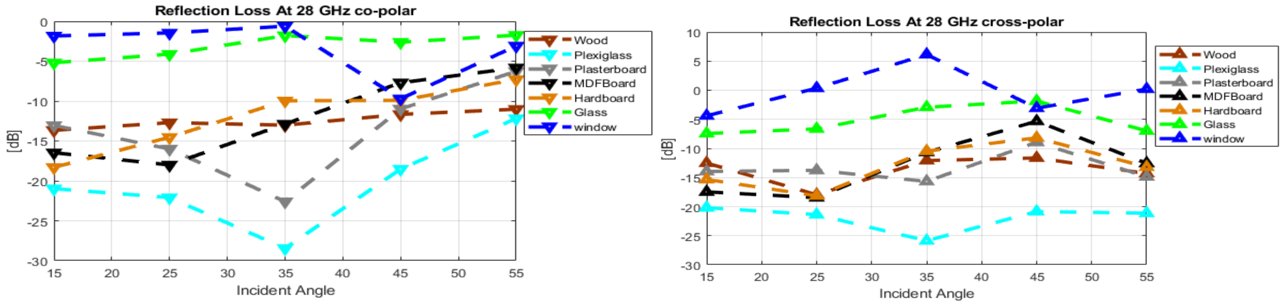

(c)

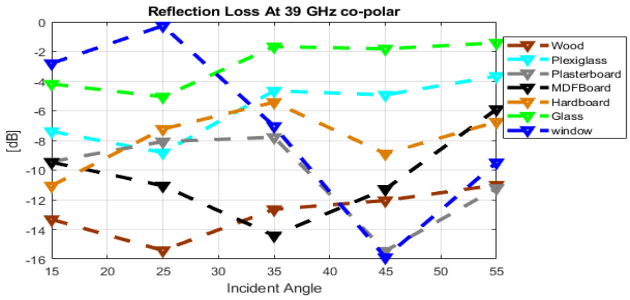


(d)

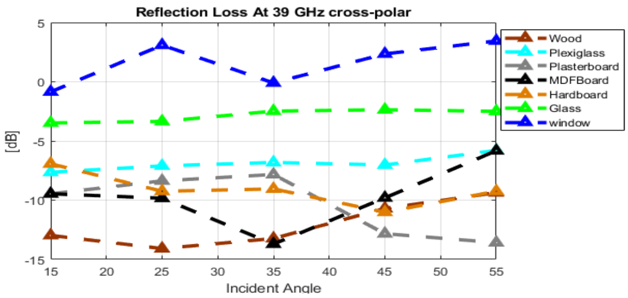


## 2.3 Conclusion

In this Report, wideband mmWave measurements performed in the 28 GHz and 39 GHz bands in co-polar (VV) and cross-polar (HV) alignments to investigate reflection and penetration loss at different incident angles are presented. The results indicate that, the lowest penetration loss value was at zero angle when both antennas of the transmitter and receiver are perpendicular on the material. In general, the penetration loss in cross-polar (HV) showed lower values compared with the co-polar (VV) alignment, where it was more than 20 dB and 30 dB in cross-polar and co-polar alignment respectively, for most of the tested materials at angles larger than 10 degrees on either side from the zero angle. For the reflection measurement results of the double-glazed window was highly reflective for both bands and in both VV and HV polarization. Furthermore, it shows at some angles higher values than the reference material in the cross-polar (HV) alignment. The reflection loss variation for all the tested materials was lower at the 39 GHz band than the 28 GHz band, where it was within 16 dB and 30 dB respectively.

## 2.4 References


[1] B. Langen, G. Lober and W. Herzig, "Reflection and transmission behaviour of building materials at 60 GHz," 5$^{th}$ IEEE International Symposium on Personal, Indoor and Mobile Radio Communications, Wireless Networks – Catching the Mobile Future, 1994, pp. 505-509 vol.2, doi: 10.1109/WNCMF.1994.529141.

[2] C. E. O. Vargas, L. S. Mello, and R. C. Rodriguez, "Measurements of construction materials penetration losses at frequencies from 26.5 GHz to 40 GHz," in IEEE Pacific Rim Conf. Communications, Computers and Signal Processing (PACRIM), Victoria, BC, Canada, 2017, pp. 1-4.

[3] H. Zhao et al., "28 GHz millimeter wave cellular communication measurements for reflection and penetration loss in and around buildings in New York City," in IEEE Int. Conf. Communications (ICC), Budapest, Hungary, 2013, pp. 5163-5167.

[4] C. E. O. Vargas and L. d. S. Mello, "Measurements of reflection and penetration loss of construction materials at 28 GHz and 38 GHz," in IEEE-APS Topical Conf. Antennas and Propagation in Wireless Communications (APWC), Cartagena des Indias, Colombia, 2018, pp. 897-900.

[5] J. Ryan, G. R. MacCartney, and T. S. Rappaport, "Indoor office wideband penetration loss measurements at 73 GHz," in IEEE Int. Conf. Communications Workshops (ICC Workshops), Paris, France, 2017, pp. 228-233.

[6] S. Salous, S. M. Feeney, X. Raimundo and A. A. Cheema, "Wideband MIMO Channel Sounder for Radio Measurements in the 60 GHz Band," in *IEEE Transactions on Wireless Communications*, vol. 15, no. 4, pp. 2825-2832, April 2016.

## 3 New measurements of glass in an anechoic chamber

Transmission loss measurements were performed on several types of glass in an anechoic chamber used 29.3 GHz band. Figure 5 shows the configuration of the measurement system, Figure 6 shows a photograph of the measurement environment, and Table 4 shows the measurement parameters. For the measurements, a horn antenna with a half power beam width of 10 degrees was installed, and the incidence angle in the horizontal plane was varied by using a rotating table, and the elevation angle in the vertical plane was varied by changing the height of the transmit and receive antennas and the distance between the transmit and receive antennas. The six types of glass used for this measurement were clear glass, patterned glass, heat reflective glass, clear wired glass, wired patterned glass, and security glass. Table 5 shows their specifications. All glass sizes are 90 cm$^2$.

FIGURE 5

**Configuration of the measurement system**

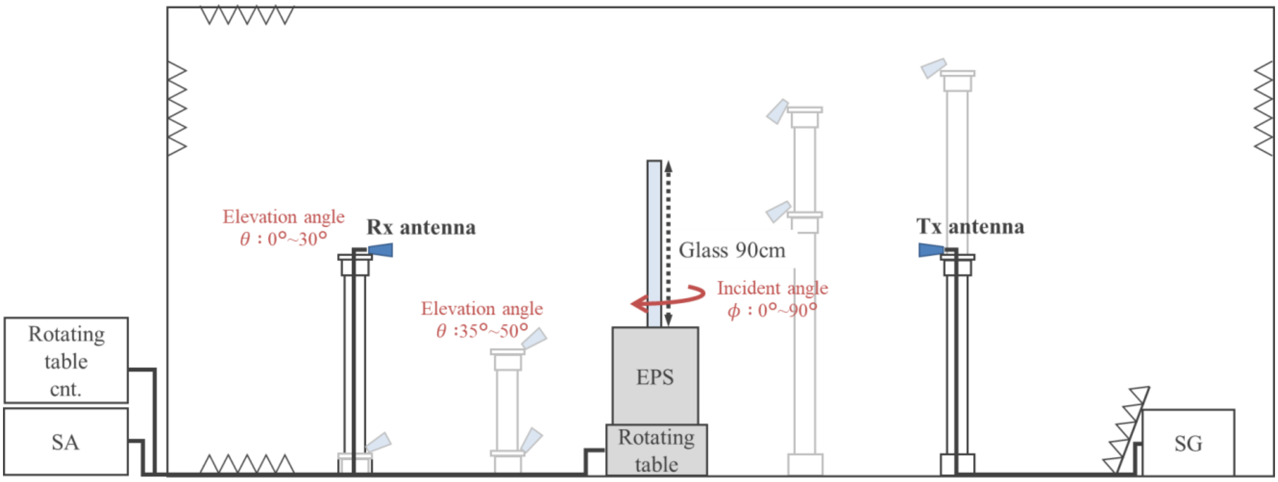


FIGURE 6

**Measurement environment**

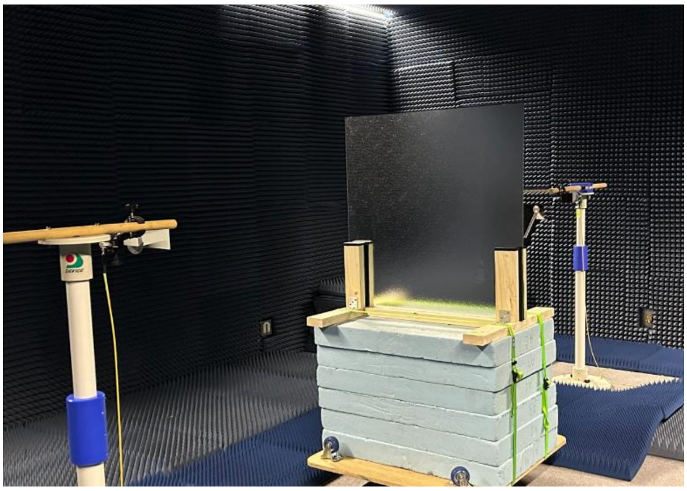

TABLE 4

**Measurement parameters**

| | |
|---|---|
| Frequency (GHz) | 29.3 |
| Transmit signal | CW |
| Antennas | Horn antenna |
| Elevation angle (degree) | 0 ~ 50 (vertical plane) |
| Incident angle (degree) | 0 ~ 90 (horizontal plane) |
| Polarizations | V-V |

TABLE 5

**Glass specifications**

| Glass types | Composition |
|---|---|
| Clear glass | 6 mm |
| Figured glass | 6 mm |
| IRR glass | ≈ 6 mm |
| Wired-clear glass | 6.8 mm |
| Wired-figured glass | 6.8 mm |
| Laminated gass | Clear glass 3 mm / PVB 60 mil / Clear glass 3 mm |
| Low-E multi-pane glass | Low-E glass 3 mm / Air 6 mm / Clear glass 3 mm |

Figure 7 shows the measurement results without glass in this measurement configuration, in other words, the loss characteristics due to the influence of the rotating table and the wooden frame that fixes the glass. From this result, it can be seen that at an elevation angle of 0 degrees, there is no effect of the rotating table and wooden frame up to an incident angle of 70 degrees, which is consistent with the free-space loss, while above an incident angle of 70°, the loss is affected by diffraction loss due to the wooden frame, which causes a fluctuation in the loss. The effective incident angles for each elevation angle are shown in Table 6.

FIGURE 7

**Measurement results without glass**

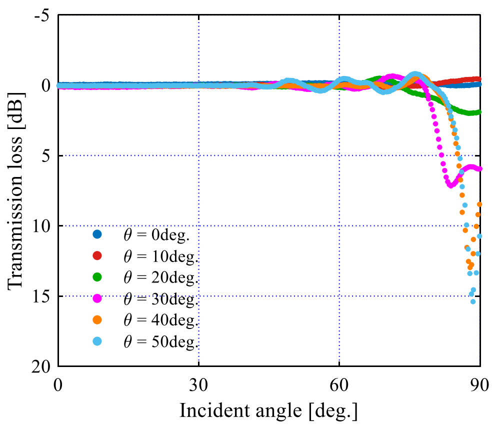

TABLE 6

**Range of effective incident angles**

| Elevation angle θ (degree) | Incident angle φ (degree) |
|---|---|
| 0 ~ 5 | 0 ~ 70 |
| 5 ~ 40 | 0 ~ 65 |
| 40 ~ 50 | 0 ~ 50 |

Figure 8 shows the measurement results of transmission loss for each glass. Although the loss characteristics are different for each glass, it was confirmed that the loss increased exponentially with an increase in the incident angle for all of the glasses.

FIGURE 8

**Measurement results**

(a) Clear glass

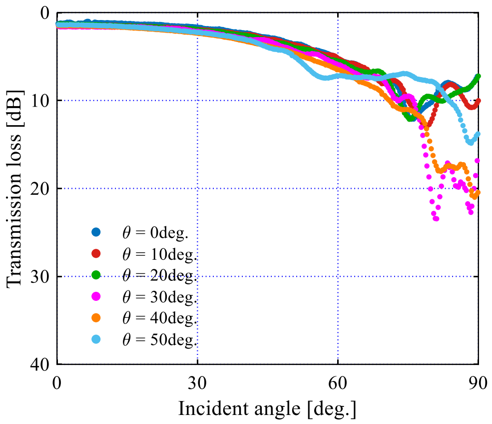


(b) Figured glass

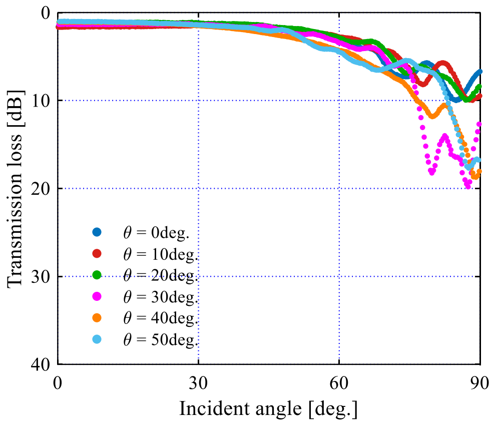


(c) IRR glass

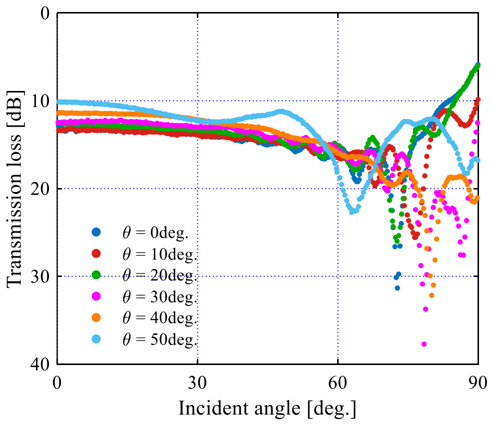


(d) Wired-clear glass

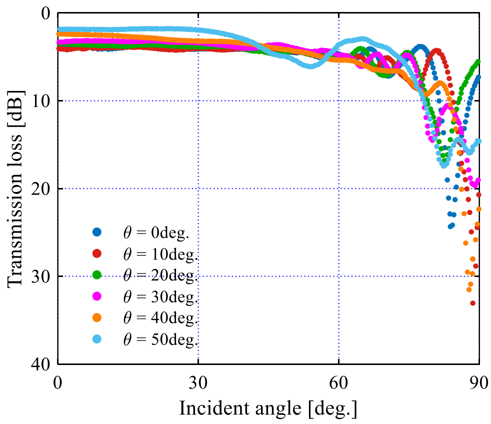

(e) Wired-figured glass

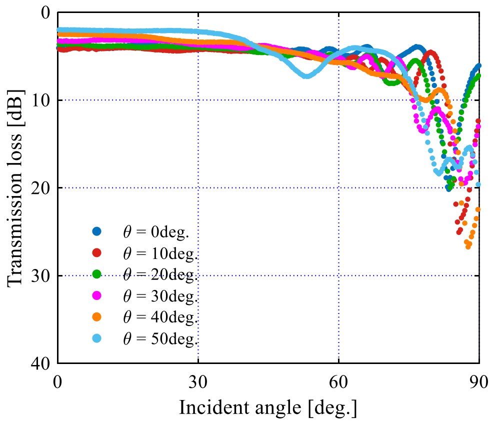


(f) Laminated glass

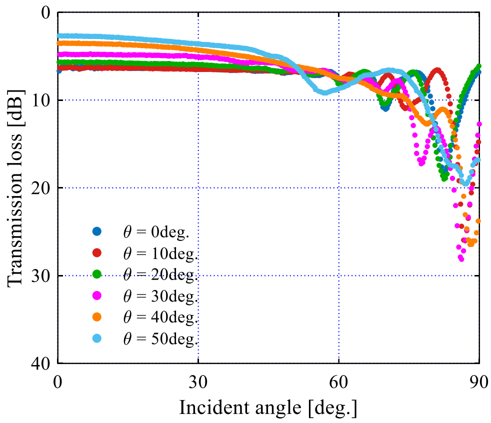


(g) Low-E multi-pane glass

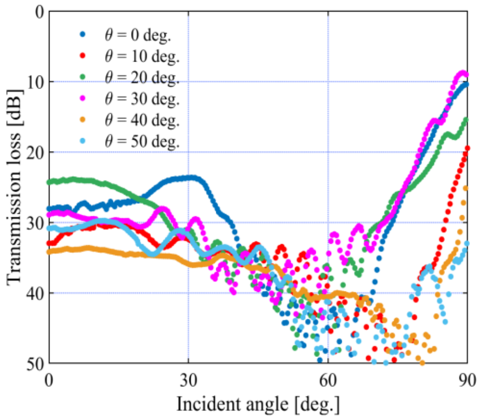


## 4 Characteristics of window penetration loss (WinPL) and its impact on BEL

### 4.1 Introduction

The importance of developing building-related propagation models and predicting propagation characteristics, such as indoor propagation and building entry loss (BEL), is steadily increasing. Furthermore, with regulations on thermally-efficient buildings becoming more stringent, most waves propagate through glass windows into or out of the building, consequently affecting propagation characteristics associated with the building. Hence, understanding the propagation properties of glass windows is crucial for characterizing and predicting indoor propagation and BEL. Recommendation ITU-R P.2040-3 provides information on various theories, such as the electrical properties of building materials, effects of material structure on radio-wave propagation, and the measured permittivity and conductivity of various materials. However, it is difficult to understand and analyse the propagation characteristics of complicated and diverse building materials with only information on permittivity and conductivity. In Report ITU-R P.2346-5, some contributions have highlighted the significant impact of the properties of glass windows on BEL characteristics. However, current ITU-R Recommendations or Reports do not provide information on propagation characteristics and frequency dependence of various types of glass windows.

This contribution presents measured results of penetration loss in the 3-40 GHz band for 13 different types of glass windows, along with an analysis of their impact on BEL.

## 4.2 Measurements

### 4.2.1 Structure and types of glass windows

In the BEL model defined in Recommendation ITU-R P.2109, building types are classified into traditional buildings and thermally-efficient buildings. This classification is based on the presence of metal coatings on windows. Single-pane, double-glazing, and triple-glazing glass windows are used, with metal coatings often applied to make the indoor room more energy efficient.

Figure 9 presents three-dimensional (3-D) structures of double- and triple- glazing windows and in bottom two-dimensional (2-D) cross-sectional structure of the glass windows. Double or triple glazed windows are constructed from a frame and a glazed unit featuring an insulating layer of Argon gas or dry air sandwiched between two panes of glass. In the cross-sectional structure of a glass window, the thickness of the glass is indicated by G and the space between the glasses is indicated by S. Glass marked with G is transparent, coloured glass is marked with CG, and glass coated with metal is marked with TeG. 13 glass windows used to measure window penetration loss (WinPL) are summarized in Table 7.

FIGURE 9

**Three-dimensional (3-D) structures of double- and triple- glazing windows (top) and two-dimensional (2-D) simple cross-sectional structure of the glass windows (bottom)**

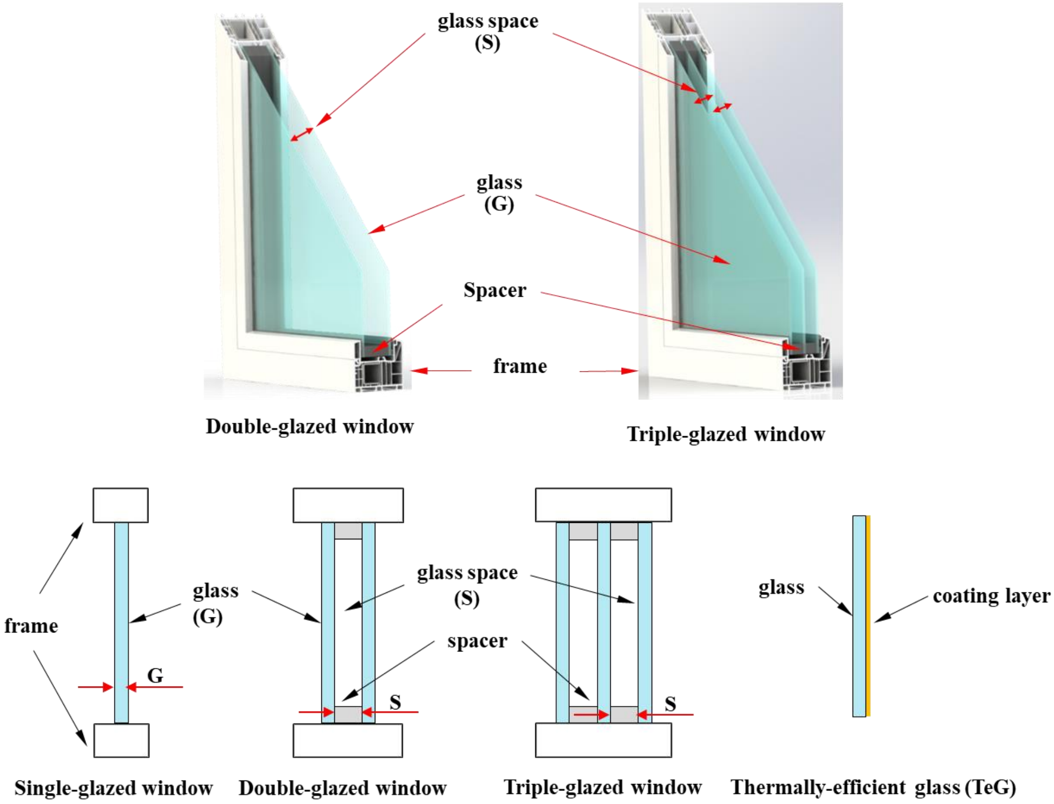

TABLE 7

**List of the glass windows for WinPL measurements**

| Structure | Type | Dimension (mm) | | Gas in space |
|---|---|---|---|---|
| Single (S) | TW | G | 5 | Air |
| Single (S) | TEW | TeG | 5 | Air |
| Double glazed (DG) | TW | G-S-G (16 mm) | 5-6-5 | Air |
| | TW | G-S-G (24 mm) | 6-12-6 | Air |
| | TEW | TeG-S-G (16 mm) | 5-6-5 | Air |
| | TEW | TeG-S-G (24 mm) | 6-12-6 | Air |
| | TEW | TeG-S-G (24 mm) | 6-12-6 | Argon |
| | TEW | TeG-S-CG (Blue) (24 mm) | 6-12-6 | Air |
| | TEW | TeG-S-CG (Blue) (24 mm) | 6-12-6 | Argon |
| Triple glazed (TG) | TEW | TeG-S-G-S-TeG (27 mm) | 5-6-5-6-5 | Air |
| | TEW | TeG-S-G-S-G (39 mm) | 5-12-5-12-5 | Air |
| | TEW | TeG-S-G-S-TeG (39 mm) | 5-12-5-12-5 | Air |

TW: traditional glass window, TEW: thermally-efficient glass window, TeG: thermally-efficient glass, CG: colour glass, S: glass space, G: transparent glass

In Table 7, types of glass windows are indicated as traditional glass windows (TW) and thermally-efficient glass windows (TEW) depending on whether they are metal-coated or not. The dimensions of the glass window are as follows. For example, a 16 mm double-glazing (DG) TW consists of two sheets of 5 mm thick glass (G) and a 6 mm wide space (S), and is indicated as G-S-G (5-6-5). Another example, a 27 mm triple-glazed (TG) TWE consists of two sheets of 5 mm thick coated glass (TeG), one sheet of 5 mm thick clear glass (G) in the centre, and a 6 mm space (S) between the panes. This configuration is denoted as TeG-S-G-S-TeG (5-6-5-6-5). It was used to compare the characteristics of glass windows filled with dry air (Air) and argon gas (Ar). Blue glass had a different dielectric constant from transparent glass due to additives added to the glass, so it was used to compare its properties.

### WinPL measurements

A setup of WinPL measurements is shown in Fig. 10. A wooden frame was designed and fabricated to support absorbers and windows. The height and width of the frame are 240 cm and 176 cm, respectively. Absorbers are attached to the frame, and an aperture for the window is located in the centre with a size of 60 cm × 60 cm. Horn antennas were installed at a height of 1.5 m at a distance of 1.0 m from the window. A signal generator (Rohde-Schwarz SMB100A and SMA 100B) and a spectrum analyser (Rohde-Schwarz FSQ40 and FSV3044) were connected to the two antennas, respectively, to measure the strength of the signal passing through the window. To measure WinPL in a wide band of 3-40 GHz, measurements were made twice in the 3-18 GHz band and the 18-40 GHz band, where each horn antenna (A-INFOMW, LB2018SF & LB-1840KF) was used in each band.

FIGURE 10

**Diagram (left) of WinPL measurements using the horn antennas (right)**

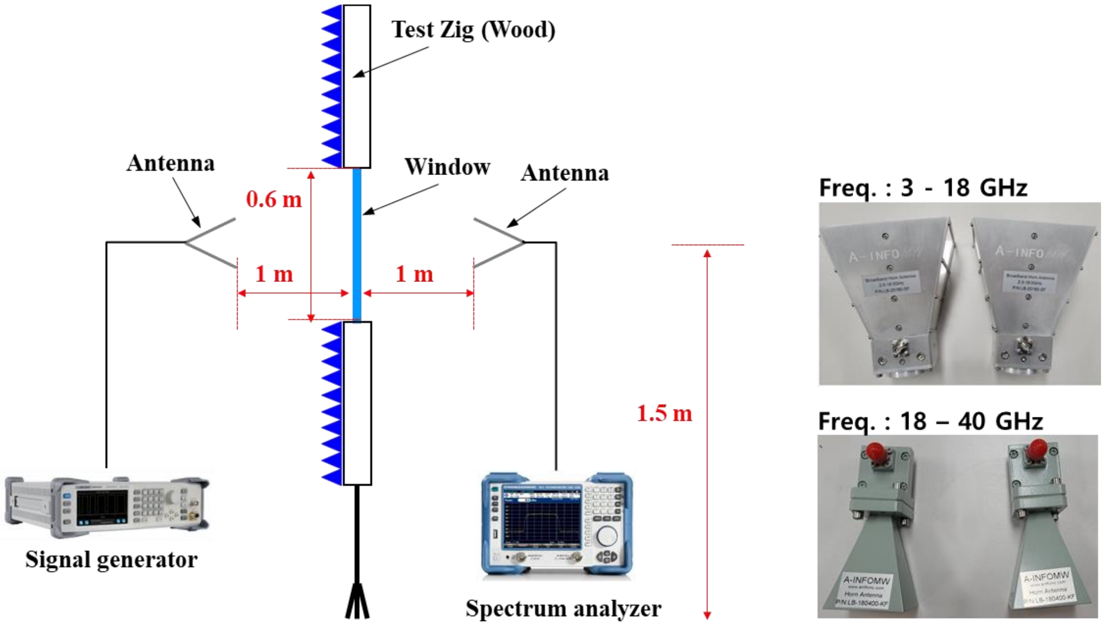


FIGURE 11

**Photographs of the setup (left) for the WinPL measurements in an anechoic chamber and aperture (right) for windows in the absorber board**

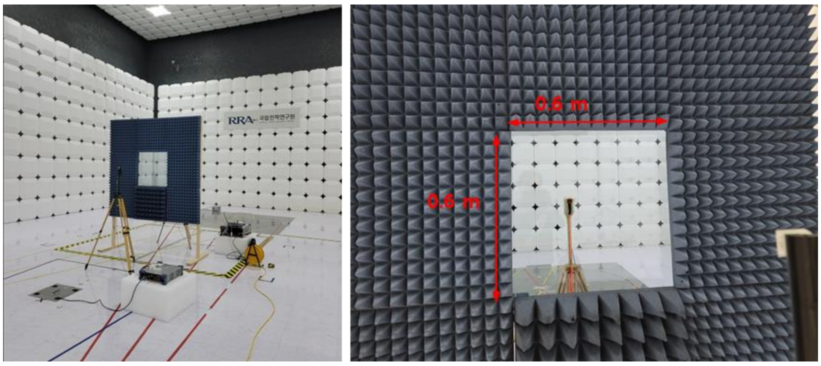


The measurements were conducted in an anechoic chamber room (National Radio Research Agency (RRA) in NaJu, Rep. of Korea) as shown in Fig. 11. The size of all glass windows used in the measurements was 76 cm × 76 cm, and the aperture size for the windows was 60 cm × 60 cm. WinPL was extracted from the difference in power measured with and without the glass window in the aperture in the centre of the absorber board. For coated single-glazed and triple-glazed windows, only the 3-30 GHz band was measured.

### Measured results

A comparison of WinPL characteristics of traditional glass windows and thermally-efficient glass windows in single-glazed, double-glazed, and triple-glazed structures is shown in Fig. 12. First, the WinPL results of 5 mm single-glazed glass traditional window (S-TW-5mm) were compared with simulation results [EM(S-TW-5mm)] using electromagnetic (EM) analysis software, and the simulation method and model are described in detail in a previously published previous literature [1]. As shown in Fig. 12, it can be seen that two results match well. As a result, it is concluded that the measurement method performed in the contribution well reflects the WinPL characteristics of glass windows.

FIGURE 12

**Comparison of WinPL characteristics of traditional glass windows and thermally efficient glass windows in single-glazed, double-glazed, and triple-glazed structures**

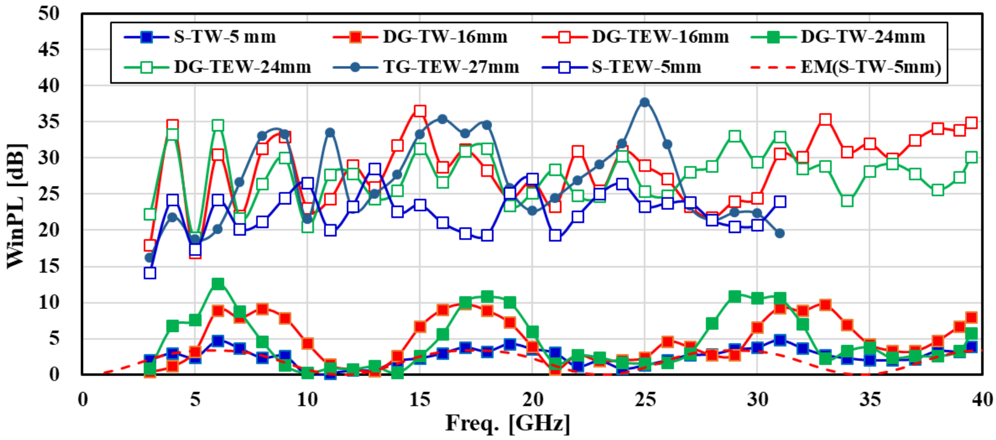


It can be seen that the WinPL of traditional glass windows (TW) and thermally-efficient glass windows (TEW) shows a clear difference. In the case of the single-glazed glass windows (S-TW-5 mm and S-TEW-5 mm), WInPL varies by about 20 dB on average depending on whether it is coated or not. Traditional glass windows exhibit periodic oscillatory characteristics depending on frequency like an odd harmonic. This is a transmission characteristic of a multilayer dielectric, and the research results were explained in detail in previous literature [1]. Despite being the double-glazed windows, their WinPL is as low as 2-3 dB in the 10-14 GHz and 22-27 GHz bands, so it can be used to select frequencies for special applications. In the case of the thermally-efficient glass windows, the WinPL is 25-30 dB on average, and a severe fluctuation of 20 dB is observed rather than a periodic oscillation according to frequency. This also has a weak correlation with the glass window structure and the thickness of the glass and space.

Figure 13 presents the WinPL characteristics of thermally efficient glass windows according to the number of coated glasses with spatial dimensions of 6 mm (left) and 12 mm (right) compared to traditional glass windows. The WinPL characteristics of a triple-pane window with a single sheet of metal-coated glass are similar to those of a double-pane window. However, it is evident that WinPL increases significantly in the case of a triple-pane window with two sheets of coated glass.

FIGURE 13

**Comparison of WinPL characteristics according to the number of coated glasses with a space dimension of 6 mm (left) and 12 mm (right)**

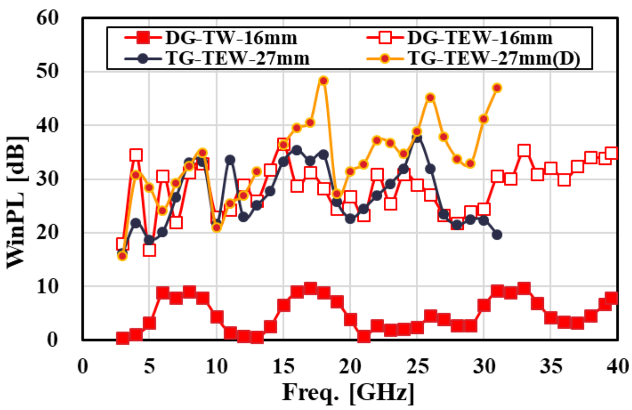


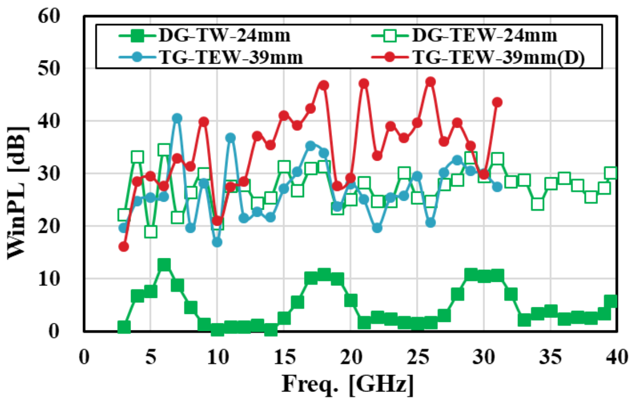

FIGURE 14

**Comparison of WinPL characteristics based on gas type in space and window colour**

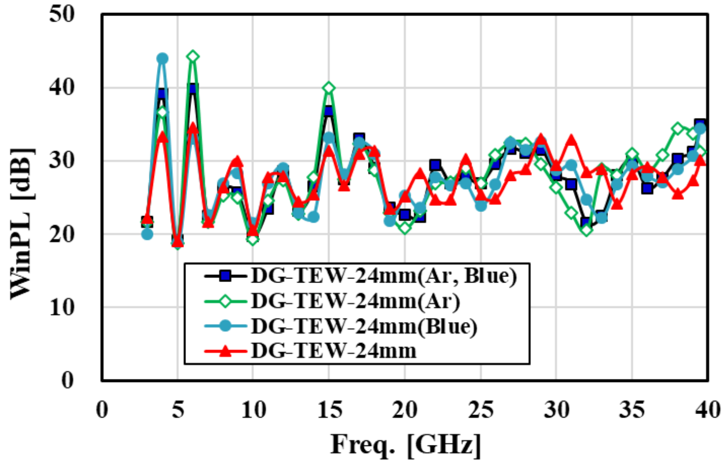


Figure 14 compares WinPL characteristics according to the type of gas in the space and window colour. Compared to a 24 mm double-glazed window (DG-TE-24mm) made of transparent glass with metal coating and filled with dry air, there is no significant difference in WinPL characteristics whether the space is filled with argon gas (Ar) instead of air or in the case of blue glass (Blue).

______________